

Hybrid high-order methods
for the numerical simulation of
elasto-acoustic wave propagation



Romain Mottier^{§†‡}

Thesis under the supervision of Alexandre Ern^{†‡} and Laurent Guillot[§]

[§] CEA, DAM, DIF, F-91297 Arpajon, France

[‡] CERMICS, Ecole des Ponts, F-77455 Marne la Vallée cedex 2

[†] SERENA Project-Team, INRIA Paris, F-75589 Paris France

Email address: romain.mottier@enpc.fr

Table of Contents

1 Motivation

- Context and issues
- Introduction to dG and HDG/HHO methods

2 Model problem

3 RK-HHO discretization

- HHO space semi-discretization
- Singly diagonally implicit schemes
- Explicit schemes

4 Numerical results

- Convergence rates
- Ricker wavelet
- Sedimentary basin

5 To go further: Unfitted HHO method

Table of Contents

1 Motivation

- Context and issues
- Introduction to dG and HDG/HHO methods

2 Model problem

3 RK-HHO discretization

- HHO space semi-discretization
- Singly diagonally implicit schemes
- Explicit schemes

4 Numerical results

- Convergence rates
- Ricker wavelet
- Sedimentary basin

5 To go further: Unfitted HHO method

Goal

Accurate modeling and simulation of seismo-acoustic waves through **heterogeneous domains with complex geometries**

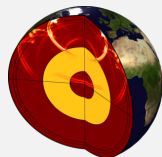


Fig. 1: Global seismic wave propagation

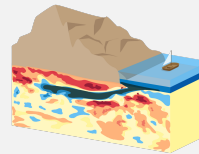


Fig. 2: Lateral heterogeneities of the earth

Goal

Accurate modeling and simulation of seismo-acoustic waves through **heterogeneous domains with complex geometries**

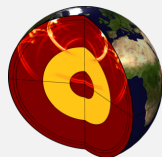


Fig. 1: Global seismic wave propagation

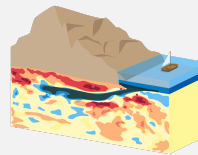


Fig. 2: Lateral heterogeneities of the earth

Issues and improvements brought by HDG/HHO methods

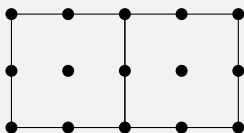
- Commonly used numerical tools: Spectral Elements Method (*e.g.* SEM3D software)
 - ▶ Hexahedral/quadrangular meshes which allow the use of tensorized polynomial basis
- **Main issue:** Complex mesh generation for classical geological structures.
- **Improvements of hybrid discontinuous methods (HDG/HHO):**
 - ▶ High-order of convergence
 - ▶ Better handling of strong property contrasts
 - ▶ Greater flexibility for time integrators

Comparison between DG and classical CG methods

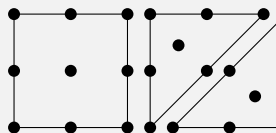
Advantages of DG methods:

- **Mesh flexibility:**
 - ▶ Complex geometries
 - ▶ Unstructured and polyhedral meshes
 - ▶ Local mesh refinement
- **Natural handling of discontinuities**
- **Broken polynomial basis:**
 - ▶ Local conservativity
- **Same order of convergence as CG**
 - ▶ H^1 -error estimate: $\mathcal{O}(h^k)$
 - ▶ L^2 -error estimate: $\mathcal{O}(h^{k+1})$

Drawbacks of DG methods: Higher computational cost and memory requirement



continuous Galerkin (CG)



Discontinuous Galerkin (DG)

Fig. 3: Distribution of discrete unknowns for CG and DG

Introduction of HDG/HHO methods

■ Seminal papers:

- ▶ HDG [Cockburn, Gopalakrishnan, Lazarovby, 2009]
- ▶ HHO [Di Pietro, Ern, Lemaire, 2014], [Di Pietro, Ern, 2015]

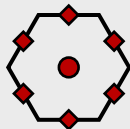
Introduction of HDG/HHO methods

■ Seminal papers:

- ▶ HDG [Cockburn, Gopalakrishnan, Lazarovby, 2009]
- ▶ HHO [Di Pietro, Ern, Lemaire, 2014], [Di Pietro, Ern, 2015]

Degrees of freedom

■ Polynomial unknowns located in the cells and on the faces



● Cell unknowns of degree k'



◆ Face unknowns of degree k

HHO unknowns:

$$\hat{u}_h := (u_{\mathcal{T}}, u_{\mathcal{F}}) \in \hat{\mathcal{U}}_h$$

Fig. 4: Local representation of HHO unknowns. **Left panel:** Equal-order discretization with $k' = k = 0$. **Right panel:** Mixed-order discretization with $k' = k + 1 = 1$.

Introduction of HDG/HHO methods

■ Seminal papers:

- ▶ HDG [Cockburn, Gopalakrishnan, Lazarovby, 2009]
- ▶ HHO [Di Pietro, Ern, Lemaire, 2014], [Di Pietro, Ern, 2015]

Degrees of freedom

■ Polynomial unknowns located in the cells and on the faces



● Cell unknowns of degree k'



◆ Face unknowns of degree k

HHO unknowns:

$$\hat{u}_h := (u_T, u_F) \in \hat{\mathcal{U}}_h$$

Fig. 4: Local representation of HHO unknowns. **Left panel:** Equal-order discretization with $k' = k = 0$. **Right panel:** Mixed-order discretization with $k' = k + 1 = 1$.

Design

- **Gradient reconstruction operator:** $(\nabla u)|_T \rightarrow \mathbf{G}_T(\hat{u}_T)$
- **Stabilization operator:** $S_{\partial T}(\delta(\hat{u}_T))$ with $\delta_{\partial T}(\hat{u}_T) := u_{T|\partial T} - u_{\partial T}$
Penalize in a least square sens

Advantages of HDG/HHO over DG methods

- Improved error estimates for smooth solutions:

- ▶ H^1 -error estimate: $\mathcal{O}(h^{k+1})$
- ▶ L^2 -error estimate: $\mathcal{O}(h^{k+2})$
(superconvergence)

- Attractive computational costs:

Elimination of cell unknowns by Schur complement (static condensation) :

- ▶ Global problem couples only face dofs
- ▶ Cell dofs recovered by local post-processing

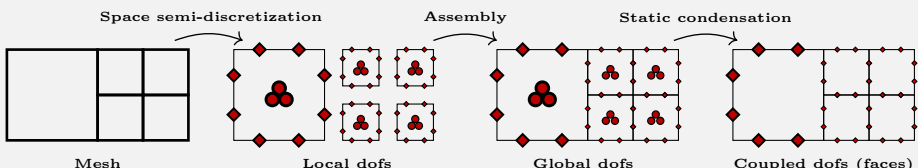


Fig. 5: Assembly and Schur complement procedure in the framework of HDG/HHO schemes

Table of Contents

1 Motivation

- Context and issues
- Introduction to dG and HDG/HHO methods

2 Model problem

3 RK-HHO discretization

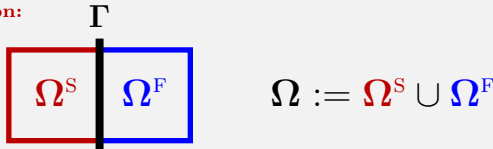
- HHO space semi-discretization
- Singly diagonally implicit schemes
- Explicit schemes

4 Numerical results

- Convergence rates
- Ricker wavelet
- Sedimentary basin

5 To go further: Unfitted HHO method

■ Domain decomposition:



$$\Omega := \Omega^S \cup \Omega^F$$

Fig. 6: Setting for elasto-acoustic coupling

■ Domain decomposition:

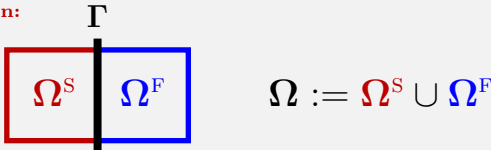


Fig. 6: Setting for elasto-acoustic coupling

Strong form of acoustic and elastic wave equation in 1st order formulation

$$\begin{cases} \partial_t \boldsymbol{\varepsilon} - \nabla_s \boldsymbol{v}^S = \mathbf{0} \\ \rho^S \partial_t \boldsymbol{v}^S - \nabla \cdot (\mathcal{C} : \boldsymbol{\varepsilon}) = \boldsymbol{f} \end{cases}$$

$$\begin{cases} \rho^F \partial_t \boldsymbol{v}^F - \nabla p = \mathbf{0} \\ \frac{1}{\kappa} \partial_t p - \nabla \cdot \boldsymbol{v}^F = g \end{cases}$$

- $\boldsymbol{v}^S \left[\frac{\text{m}}{\text{s}} \right]$ elastic velocity field
- $\boldsymbol{\varepsilon} := \nabla_s u$ linearized strain tensor
- $\rho^S \left[\frac{\text{kg}}{\text{m}^3} \right]$ solid density
- \mathcal{C} [Pa] 4th-order Hooke tensor
- $\boldsymbol{f} \left[\frac{\text{kg}}{\text{m}^2 \text{s}^2} \right]$ source term
- p [Pa] scalar pressure field
- $\boldsymbol{v}^F \left[\frac{\text{m}}{\text{s}} \right]$ acoustic velocity field
- $\rho^F \left[\frac{\text{kg}}{\text{m}^3} \right]$ fluid density
- κ [Pa] fluid bulk modulus
- $g \left[\frac{1}{\text{s}} \right]$ source term

■ Domain decomposition:

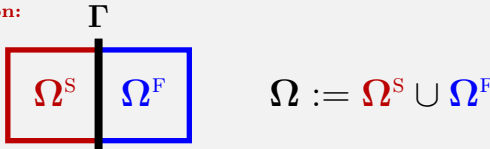


Fig. 6: Setting for elasto-acoustic coupling

Strong form of acoustic and elastic wave equation in 1st order formulation

$$\begin{cases} \partial_t \boldsymbol{\varepsilon} - \nabla_s \boldsymbol{v}^S = \mathbf{0} \\ \rho^S \partial_t \boldsymbol{v}^S - \nabla \cdot (\mathcal{C} : \boldsymbol{\varepsilon}) = \boldsymbol{f} \end{cases}$$

$$\begin{cases} \rho^F \partial_t \boldsymbol{v}^F - \nabla p = \mathbf{0} \\ \frac{1}{\kappa} \partial_t p - \nabla \cdot \boldsymbol{v}^F = g \end{cases}$$

- $\boldsymbol{v}^S \left[\frac{\text{m}}{\text{s}} \right]$ elastic velocity field
- $\boldsymbol{\varepsilon} := \nabla_s u$ linearized strain tensor
- $\rho^S \left[\frac{\text{kg}}{\text{m}^3} \right]$ solid density
- \mathcal{C} [Pa] 4th-order Hooke tensor
- $\boldsymbol{f} \left[\frac{\text{kg}}{\text{m}^2 \text{s}^2} \right]$ source term
- p [Pa] scalar pressure field
- $\boldsymbol{v}^F \left[\frac{\text{m}}{\text{s}} \right]$ acoustic velocity field
- $\rho^F \left[\frac{\text{kg}}{\text{m}^3} \right]$ fluid density
- κ [Pa] fluid bulk modulus
- $g \left[\frac{1}{\text{s}} \right]$ source term

Coupling conditions

$$\begin{cases} \boldsymbol{v}^S \cdot \mathbf{n}_\Gamma = \boldsymbol{v}^F \cdot \mathbf{n}_\Gamma \\ (\mathcal{C} : \boldsymbol{\varepsilon}) \cdot \mathbf{n}_\Gamma = p \mathbf{n}_\Gamma \end{cases}$$

- Continuity of the velocity's normal component
- Balance of forces

Initial and boundary conditions

■ Acoustic domain:

$$\begin{aligned} p|_{t=0} &= p_0 && \text{in } \Omega^F, & p|_{\partial\Omega^F \setminus \Gamma} &= 0 && \text{on } J \times (\partial\Omega^F \setminus \Gamma). \\ \boldsymbol{v}^F|_{t=0} &= \boldsymbol{v}_0^F && \end{aligned}$$

■ Elastic domain:

$$\begin{aligned} \boldsymbol{v}^S|_{t=0} &= \boldsymbol{v}_0^S && \text{in } \Omega^S, & \boldsymbol{v}^S|_{\partial\Omega^S \setminus \Gamma} &= \mathbf{0} && \text{on } J \times (\partial\Omega^S \setminus \Gamma). \\ \boldsymbol{\varepsilon}|_{t=0} &= \boldsymbol{\varepsilon}_0 && \end{aligned}$$

■ Homogeneous Dirichlet boundary conditions on $\partial\Omega$ for simplicity

Initial and boundary conditions

■ Acoustic domain:

$$\begin{aligned} p|_{t=0} &= p_0 && \text{in } \Omega^F, \\ \mathbf{v}^F|_{t=0} &= \mathbf{v}_0^F && p|_{\partial\Omega^F \setminus \Gamma} = 0 && \text{on } J \times (\partial\Omega^F \setminus \Gamma). \end{aligned}$$

■ Elastic domain:

$$\begin{aligned} \mathbf{v}^S|_{t=0} &= \mathbf{v}_0^S && \text{in } \Omega^S, \\ \boldsymbol{\epsilon}|_{t=0} &= \boldsymbol{\epsilon}_0 && \mathbf{v}^S|_{\partial\Omega^S \setminus \Gamma} = \mathbf{0} && \text{on } J \times (\partial\Omega^S \setminus \Gamma). \end{aligned}$$

■ Homogeneous Dirichlet boundary conditions on $\partial\Omega$ for simplicityWeak form of the acoustic and elastic wave equations in 1st order formulation

■ Let $J := (0, T_f)$ with $T_f > 0$

■ **Acoustic:** Find $(p, \mathbf{v}^F) : J \times \Omega^F \rightarrow \mathbb{R} \times \mathbb{R}^d$ such that, for all $t \in J$,

$$\begin{cases} \rho^F(\partial_t \mathbf{v}^F(t), \mathbf{q})_{\Omega^F} - (\nabla p(t), \mathbf{q})_{\Omega^F} = 0, \\ \frac{1}{\kappa}(\partial_t p(t), r)_{\Omega^F} + (\mathbf{v}^F(t), \nabla r)_{\Omega^F} + (\mathbf{v}^S(t) \cdot \mathbf{n}_\Gamma, r)_\Gamma = (g(t), r)_{\Omega^F}, \end{cases}$$

$$\forall (r, \mathbf{q}) \in H_{0F}^1(\Omega^F) \times \mathbf{L}^2(\Omega^F).$$

■ **Elastic:** Find $(\mathbf{v}^S, \boldsymbol{\epsilon}) : J \times \Omega^S \rightarrow \mathbb{R}^d \times \mathbb{R}_{\text{sym}}^{d \times d}$ such that, for all $t \in J$,

$$\begin{cases} (\partial_t \boldsymbol{\epsilon}(t), \mathbf{z})_{\Omega^S} - (\nabla_s \mathbf{v}^S(t), \mathbf{z})_{\Omega^S} = 0, \\ \rho^S(\partial_t \mathbf{v}^S(t), \mathbf{w})_{\Omega^S} + (\mathcal{C} : \boldsymbol{\epsilon}(t), \nabla_s \mathbf{w})_{\Omega^S} - (p(t) \mathbf{n}_\Gamma, \mathbf{w})_\Gamma = (\mathbf{f}(t), \mathbf{w})_{\Omega^S}, \end{cases}$$

$$\forall (\mathbf{w}, \mathbf{z}) \in \mathbf{H}_{0S}^1(\Omega^S) \times \mathbf{L}^2(\Omega^S; \mathbb{R}_{\text{sym}}^{d \times d}).$$

Table of Contents

1 Motivation

- Context and issues
- Introduction to dG and HDG/HHO methods

2 Model problem

3 RK-HHO discretization

- HHO space semi-discretization
- Singly diagonally implicit schemes
- Explicit schemes

4 Numerical results

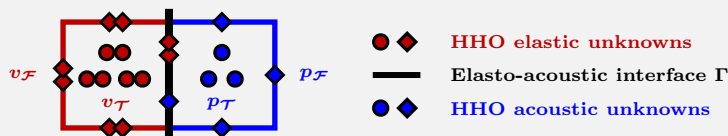
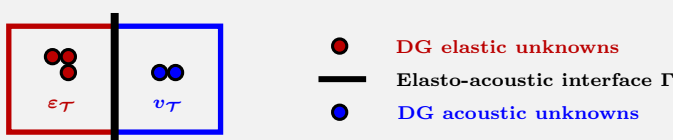
- Convergence rates
- Ricker wavelet
- Sedimentary basin

5 To go further: Unfitted HHO method

Approximation spaces and HHO space semi-discretization

■ **Acoustic domain:** $\mathcal{V}_{\mathcal{T}^F}^k := \underbrace{\bigtimes_{T \in \mathcal{T}_h^F} \mathbb{P}^k(T; \mathbb{R}^d)}_{\text{space for } \mathbf{v}^F}, \quad \widehat{\mathcal{U}}_h^F := \underbrace{\bigtimes_{T \in \mathcal{T}_h^F} \mathbb{P}^{k'}(T; \mathbb{R}) \times \bigtimes_{F \in \mathcal{F}_h^F} \mathbb{P}^k(F; \mathbb{R})}_{\text{space for } p}$

■ **Elastic domain:** $\mathcal{Z}_{\mathcal{T}^S}^k := \underbrace{\bigtimes_{T \in \mathcal{T}_h^S} \mathbb{P}^k(T; \mathbb{R}_{\text{sym}}^{d \times d})}_{\text{space for } \boldsymbol{\epsilon}}, \quad \widehat{\mathcal{U}}_h^S := \underbrace{\bigtimes_{T \in \mathcal{T}_h^S} \mathbb{P}^{k'}(T; \mathbb{R}^d) \times \bigtimes_{F \in \mathcal{F}_h^S} \mathbb{P}^k(F; \mathbb{R}^d)}_{\text{space for } \mathbf{v}^S}$

Fig. 7: Elasto-acoustic HHO unknowns with $k' = 1, k = 0$.Fig. 8: Elasto-acoustic DG unknowns with $k = 0$.

Local reconstruction operators

■ Acoustic domain: Gradient reconstruction:

$\mathbf{G}_T : \widehat{\mathcal{U}}_T^F \rightarrow \mathbb{P}^k(T; \mathbb{R}^d)$ is s.t. for all $\hat{p}_T \in \widehat{\mathcal{U}}_T^F$,

$$(\mathbf{G}_T(\hat{p}_T), \mathbf{q})_T = (\nabla p_T, \mathbf{q})_T - (p_T - p_{\partial T}, \mathbf{q} \cdot \mathbf{n}_T)_{\partial T}, \quad \forall \mathbf{q} \in \mathbb{P}^k(T; \mathbb{R}^d)$$

■ Elastic domain: Strain reconstruction

$\mathbf{E}_T : \widehat{\mathcal{U}}_T^S \rightarrow \mathbb{P}^k(T; \mathbb{R}_{\text{sym}}^{d \times d})$ s.t. for all $\hat{\mathbf{v}}_T^S \in \widehat{\mathcal{U}}_T^S$ and all $\boldsymbol{\zeta} \in \mathbb{P}^k(T; \mathbb{R}_{\text{sym}}^{d \times d})$,

$$(\mathbf{E}_T(\hat{\mathbf{v}}_T^S), \boldsymbol{\zeta})_T = (\nabla_s \mathbf{v}_T^S, \boldsymbol{\zeta})_T - (\mathbf{v}_T^S - \mathbf{v}_{\partial T}^S, \boldsymbol{\zeta} \cdot \mathbf{n}_T)_{\partial T}$$

Local reconstruction operators

■ Acoustic domain: Gradient reconstruction:

$\mathbf{G}_T : \widehat{\mathcal{U}}_T^F \rightarrow \mathbb{P}^k(T; \mathbb{R}^d)$ is s.t. for all $\hat{p}_T \in \widehat{\mathcal{U}}_T^F$,

$$(\mathbf{G}_T(\hat{p}_T), \mathbf{q})_T = (\nabla p_T, \mathbf{q})_T - (p_T - p_{\partial T}, \mathbf{q} \cdot \mathbf{n}_T)_{\partial T}, \quad \forall \mathbf{q} \in \mathbb{P}^k(T; \mathbb{R}^d)$$

■ Elastic domain: Strain reconstruction

$\mathbf{E}_T : \widehat{\mathcal{U}}_T^S \rightarrow \mathbb{P}^k(T; \mathbb{R}_{\text{sym}}^{d \times d})$ s.t. for all $\hat{\mathbf{v}}_T^S \in \widehat{\mathcal{U}}_T^S$ and all $\zeta \in \mathbb{P}^k(T; \mathbb{R}_{\text{sym}}^{d \times d})$,

$$(\mathbf{E}_T(\hat{\mathbf{v}}_T^S), \zeta)_T = (\nabla_s \mathbf{v}_T^S, \zeta)_T - (\mathbf{v}_T^S - \mathbf{v}_{\partial T}^S, \zeta \cdot \mathbf{n}_T)_{\partial T}$$

Local stabilization operators

■ Mixed-order discretization: Same stabilization as HDG (Lehrenfeld-Schöberl)

$$S_{\partial T}(\delta(\hat{p}_h)) := \Pi_{\partial T}^k(\delta(\hat{p}_h)) \quad S_{\partial T}(\boldsymbol{\delta}(\hat{\mathbf{v}}_h^S)) := \boldsymbol{\Pi}_{\partial T}^k(\boldsymbol{\delta}(\hat{\mathbf{v}}_h^S))$$

■ Equal-order discretization: Specific stabilization to HHO

$$S_{\partial T}(\delta(\hat{p}_h)) := \Pi_{\partial T}^k(\delta(\hat{p}_h)) + ((I - \Pi_T^k)R_T(0, \delta(\hat{p}_h)))|_{\partial T}$$

$$S_{\partial T}(\boldsymbol{\delta}(\hat{\mathbf{v}}_h^S)) := \boldsymbol{\Pi}_{\partial T}^k(\boldsymbol{\delta}(\hat{\mathbf{v}}_h^S)) + ((\mathbf{I} - \boldsymbol{\Pi}_T^k)\mathbf{R}_T(0, \boldsymbol{\delta}(\hat{\mathbf{v}}_h^S)))|_{\partial T}$$

- ▶ More costly than the mixed-order case
- ▶ Need additional velocity and pressure reconstructions (R_T and \mathbf{R}_T)

Global operators

■ Global gradient reconstructions:

$$\mathbf{G}_{\mathcal{T}} : \widehat{\mathcal{U}}_h^F \rightarrow \bigtimes_{T \in \mathcal{T}_h} \mathbb{P}^k(T; \mathbb{R}^d) \text{ s.t. } (\mathbf{G}_{\mathcal{T}}(\hat{p}_h))|_T := \mathbf{G}_T(\hat{p}_T) \text{ for all } T \in \mathcal{T}_h \text{ and all } \hat{p}_h \in \widehat{\mathcal{U}}_h^F$$

$$\mathbf{E}_{\mathcal{T}} : \widehat{\mathcal{U}}_h^S \rightarrow \bigtimes_{T \in \mathcal{T}_h} \mathbb{P}^k(T; \mathbb{R}_{\text{sym}}^{d \times d}) \text{ s.t. } (\mathbf{E}_{\mathcal{T}}(\hat{\mathbf{v}}_h^S))|_T := \mathbf{E}_T(\hat{\mathbf{v}}_T^S) \text{ for all } T \in \mathcal{T}_h \text{ and all } \hat{\mathbf{v}}_h^S \in \widehat{\mathcal{U}}_h^S$$

■ Global stabilization forms:

For all $T \in \mathcal{T}_h$,

$$s_h^F(\hat{p}_h, \hat{q}_h) = \sum_{T \in \mathcal{T}_h} \tau_T^F(\mathbf{S}_{\partial T}(\hat{p}_h), \mathbf{S}_{\partial T}(\hat{q}_h))_{\partial T}$$

$$s_h^S(\hat{\mathbf{v}}_h^S, \hat{\boldsymbol{\zeta}}_h) = \sum_{T \in \mathcal{T}_h} \tau_T^S(\mathbf{S}_{\partial T}(\hat{\mathbf{v}}_h^S), \mathbf{S}_{\partial T}(\hat{\boldsymbol{\zeta}}_h))_{\partial T}$$

Global operators

■ Global gradient reconstructions:

$$\mathbf{G}_{\mathcal{T}} : \widehat{\mathcal{U}}_h^F \rightarrow \bigtimes_{T \in \mathcal{T}_h} \mathbb{P}^k(T; \mathbb{R}^d) \text{ s.t. } (\mathbf{G}_{\mathcal{T}}(\hat{p}_h))|_T := \mathbf{G}_T(\hat{p}_T) \text{ for all } T \in \mathcal{T}_h \text{ and all } \hat{p}_h \in \widehat{\mathcal{U}}_h^F$$

$$\mathbf{E}_{\mathcal{T}} : \widehat{\mathcal{U}}_h^S \rightarrow \bigtimes_{T \in \mathcal{T}_h} \mathbb{P}^k(T; \mathbb{R}_{\text{sym}}^{d \times d}) \text{ s.t. } (\mathbf{E}_{\mathcal{T}}(\hat{\mathbf{v}}_h^S))|_T := \mathbf{E}_T(\hat{\mathbf{v}}_T^S) \text{ for all } T \in \mathcal{T}_h \text{ and all } \hat{\mathbf{v}}_h^S \in \widehat{\mathcal{U}}_h^S$$

■ Global stabilization forms:

For all $T \in \mathcal{T}_h$,

$$s_h^F(\hat{p}_h, \hat{q}_h) = \sum_{T \in \mathcal{T}_h} \tau_T^F (\mathbf{S}_{\partial T}(\hat{p}_h), \mathbf{S}_{\partial T}(\hat{q}_h))_{\partial T}$$

$$s_h^S(\hat{\mathbf{v}}_h^S, \hat{\boldsymbol{\zeta}}_h) = \sum_{T \in \mathcal{T}_h} \tau_T^S (\mathbf{S}_{\partial T}(\hat{\mathbf{v}}_h^S), \mathbf{S}_{\partial T}(\hat{\boldsymbol{\zeta}}_h))_{\partial T}$$

Stabilization parameter

■ Acoustic stabilization parameter:

$$\blacktriangleright \tau_T^F := \frac{1}{\rho_F c_P^F} = \mathcal{O}(1) \quad \blacktriangleright \tau_T^F := \frac{1}{\rho_F c_P^F} \frac{\ell_\Omega}{h_T} = \mathcal{O}(h_T^{-1})$$

■ Elastic stabilization parameter:

$$\blacktriangleright \tau_T^S := \rho_S^S c_S = \mathcal{O}(1) \quad \blacktriangleright \tau_T^S := \rho_S^S c_S \frac{\ell_\Omega}{h_T} = \mathcal{O}(h_T^{-1})$$

■ Dimensionnaly consistent parameter

HHO space semi-discretization for the elasto-acoustic coupling

■ Acoustic wave equation:

$$(\rho^F \partial_t \mathbf{v}_{\mathcal{T}^F}(t), \mathbf{r}_\tau)_{\Omega^F} + (\mathbf{G}_\tau(\hat{p}_h(t)), \mathbf{r}_\tau)_{\Omega^F} = 0$$

$$\left(\frac{1}{\kappa} \partial_t p_\tau(t), q_\tau \right)_{\Omega^F} - (\mathbf{v}_{\mathcal{T}^F}(t), \mathbf{G}_\tau(\hat{q}_h))_{\Omega^F} + s_h^F(\hat{p}_h(t), \hat{q}_h) - (\mathbf{v}_{\mathcal{F}^S}^S(t) \cdot \mathbf{n}_\Gamma, q_\mathcal{F})_\Gamma = (g(t), q_\tau)_{\Omega^F}$$

■ Elastic wave equation:

$$(\partial_t \boldsymbol{\varepsilon}_\tau(t), \mathbf{z}_\tau)_{\Omega^S} - (\mathbf{E}_\tau(\hat{\mathbf{v}}_h^S(t)), \mathbf{z}_\tau)_{\Omega^S} = 0$$

$$(\rho^S \partial_t \mathbf{v}_{\mathcal{T}^S}^S(t), \mathbf{w}_\tau)_{\Omega^S} + (\mathbf{C} : \boldsymbol{\varepsilon}_\tau, \mathbf{E}_\tau(\hat{\mathbf{w}}_h))_{\Omega^S} + s_h^S(\hat{\mathbf{v}}_h^S, \hat{\mathbf{w}}_h) + (p_\mathcal{F}(t), \mathbf{w}_\mathcal{F} \cdot \mathbf{n}_\Gamma)_\Gamma = (\mathbf{f}(t), \mathbf{w}_\tau)_{\Omega^S}$$

HHO space semi-discretization for the elasto-acoustic coupling

■ Acoustic wave equation:

$$(\rho^F \partial_t \mathbf{v}_{\mathcal{T}^F}(t), \mathbf{r}_{\mathcal{T}})_{\Omega^F} + (\mathbf{G}_{\mathcal{T}}(\hat{p}_h(t)), \mathbf{r}_{\mathcal{T}})_{\Omega^F} = 0$$

$$\left(\frac{1}{\kappa} \partial_t p_{\mathcal{T}}(t), q_{\mathcal{T}} \right)_{\Omega^F} - (\mathbf{v}_{\mathcal{T}^F}(t), \mathbf{G}_{\mathcal{T}}(\hat{q}_h))_{\Omega^F} + s_h^F(\hat{p}_h(t), \hat{q}_h) - (\mathbf{v}_{\mathcal{T}^S}^S(t) \cdot \mathbf{n}_{\Gamma}, q_{\mathcal{F}})_{\Gamma} = (g(t), q_{\mathcal{T}})_{\Omega^F}$$

■ Elastic wave equation:

$$(\partial_t \boldsymbol{\varepsilon}_{\mathcal{T}}(t), \mathbf{z}_{\mathcal{T}})_{\Omega^S} - (\mathbf{E}_{\mathcal{T}}(\hat{\mathbf{v}}_h^S(t)), \mathbf{z}_{\mathcal{T}})_{\Omega^S} = 0$$

$$(\rho^S \partial_t \mathbf{v}_{\mathcal{T}^S}(t), \mathbf{w}_{\mathcal{T}})_{\Omega^S} + (\mathbf{C} : \boldsymbol{\varepsilon}_{\mathcal{T}}, \mathbf{E}_{\mathcal{T}}(\hat{\mathbf{w}}_h))_{\Omega^S} + s_h^S(\hat{\mathbf{v}}_h^S, \hat{\mathbf{w}}_h) + (p_{\mathcal{F}}(t), \mathbf{w}_{\mathcal{F}} \cdot \mathbf{n}_{\Gamma})_{\Gamma} = (\mathbf{f}(t), \mathbf{w}_{\mathcal{T}})_{\Omega^S}$$

Energy balance

■ Mechanical energy of the scheme: $\mathcal{E}_h(t) := \mathcal{E}_h^S(t) + \mathcal{E}_h^F(t)$ with

$$\mathcal{E}_h^F(t) := \frac{1}{2} \|\rho^F \mathbf{v}_{\mathcal{T}^F}(t)\|_{\Omega^F}^2 + \frac{1}{2} \left\| \frac{1}{\kappa} p_{\mathcal{T}}(t) \right\|_{\Omega^F}^2$$

$$\mathcal{E}_h^S(t) := \frac{1}{2} \|\rho^S \mathbf{v}_{\mathcal{T}^S}(t)\|_{\Omega^S}^2 + \frac{1}{2} \|\mathbf{C} : \boldsymbol{\varepsilon}(t)\|_{\Omega^S}^2$$

■ Semi-discrete energy conservation of the scheme:

$$\begin{aligned} \mathcal{E}_h(t) + \int_0^t \left[s_h^S(\hat{\mathbf{v}}_h^S(\alpha), \hat{\mathbf{v}}_h^S(\alpha)) + s_h^F(\hat{p}_h(\alpha), \hat{p}_h(\alpha)) \right] d\alpha = \\ \mathcal{E}_h(0) + \int_0^t \left[(\mathbf{f}(\alpha), \mathbf{v}_{\mathcal{T}^S}^S(\alpha))_{\Omega^S} + (g(\alpha), p_{\mathcal{T}}(\alpha))_{\Omega^F} \right] d\alpha \end{aligned}$$

► 1st order formulation: stabilisation dissipates exact energy

Algebraic realization

- Static coupling between cell and face unknowns

$$\left[\begin{array}{ccc|ccc} \mathbf{M}_{\mathcal{T}\mathcal{T}}^{v^F} & 0 & 0 & 0 & 0 & 0 \\ 0 & \mathbf{M}_{\mathcal{T}\mathcal{T}}^F & 0 & 0 & 0 & 0 \\ 0 & 0 & 0 & 0 & 0 & 0 \end{array} \right] \frac{d}{dt} \begin{bmatrix} \mathbf{V}_{\mathcal{T}^F}^F \\ \mathbf{P}_{\mathcal{T}^F} \\ \mathbf{P}_{\mathcal{F}^F} \end{bmatrix} + \left[\begin{array}{ccc|ccc} 0 & -G_{\mathcal{T}} & -G_{\mathcal{F}} & 0 & 0 & 0 \\ G_{\mathcal{T}}^\dagger & \Sigma_{\mathcal{T}\mathcal{T}}^F & \Sigma_{\mathcal{T}\mathcal{F}}^F & 0 & 0 & 0 \\ G_{\mathcal{F}}^\dagger & \Sigma_{\mathcal{F}\mathcal{T}}^F & \Sigma_{\mathcal{F}\mathcal{F}}^F & 0 & 0 & C_\Gamma \end{array} \right] \begin{bmatrix} \mathbf{V}_{\mathcal{T}^F}^F \\ \mathbf{P}_{\mathcal{T}^F} \\ \mathbf{P}_{\mathcal{F}^F} \end{bmatrix} = \left[\begin{array}{c} 0 \\ G_{\mathcal{T}^F} \\ 0 \end{array} \right]$$

$$\left[\begin{array}{ccc|ccc} 0 & 0 & 0 & \mathbf{M}_{\mathcal{T}\mathcal{T}}^{\epsilon} & 0 & 0 \\ 0 & 0 & 0 & 0 & \mathbf{M}_{\mathcal{T}\mathcal{T}}^S & 0 \\ 0 & 0 & 0 & 0 & 0 & 0 \end{array} \right] \frac{d}{dt} \begin{bmatrix} \mathbf{S}_{\mathcal{T}^s} \\ \mathbf{V}_{\mathcal{T}^s}^S \\ \mathbf{V}_{\mathcal{F}^s}^S \end{bmatrix} + \left[\begin{array}{ccc|ccc} 0 & 0 & 0 & 0 & -E_{\mathcal{T}} & -E_{\mathcal{F}} \\ 0 & 0 & 0 & E_{\mathcal{T}}^\dagger & \Sigma_{\mathcal{T}\mathcal{T}}^S & \Sigma_{\mathcal{T}\mathcal{F}}^S \\ 0 & 0 & 0 & E_{\mathcal{F}}^\dagger & \Sigma_{\mathcal{F}\mathcal{T}}^S & \Sigma_{\mathcal{F}\mathcal{F}}^S \end{array} \right] \begin{bmatrix} \mathbf{S}_{\mathcal{T}^s} \\ \mathbf{V}_{\mathcal{T}^s}^S \\ \mathbf{V}_{\mathcal{F}^s}^S \end{bmatrix} = \left[\begin{array}{c} 0 \\ 0 \\ F_{\mathcal{T}^s} \end{array} \right]$$

Algebraic realization

- Static coupling between cell and face unknowns

$$\left[\begin{array}{cc|cc|c} \mathbf{M}_{\mathcal{T}\mathcal{T}}^{v^F} & 0 & 0 & 0 & 0 \\ 0 & \mathbf{M}_{\mathcal{T}\mathcal{T}}^F & 0 & 0 & 0 \\ 0 & 0 & 0 & 0 & 0 \\ \hline 0 & 0 & 0 & \mathbf{M}_{\mathcal{T}\mathcal{T}}^\epsilon & 0 \\ 0 & 0 & 0 & 0 & \mathbf{M}_{\mathcal{T}\mathcal{T}}^S \\ 0 & 0 & 0 & 0 & 0 \end{array} \right] \frac{d}{dt} \left[\begin{array}{c} \mathbf{V}_{\mathcal{T}^F} \\ \mathbf{P}_{\mathcal{T}^F} \\ \mathbf{P}_{\mathcal{F}^F} \\ \hline \mathbf{S}_{\mathcal{T}^S} \\ \mathbf{V}_{\mathcal{T}^S}^S \\ \mathbf{V}_{\mathcal{F}^S}^S \end{array} \right] + \left[\begin{array}{ccc|ccc} 0 & -G_{\mathcal{T}} & -G_{\mathcal{F}} & 0 & 0 & 0 \\ G_{\mathcal{T}}^\dagger & \Sigma_{\mathcal{T}\mathcal{T}}^F & \Sigma_{\mathcal{T}\mathcal{F}}^F & 0 & 0 & 0 \\ G_{\mathcal{F}}^\dagger & \Sigma_{\mathcal{F}\mathcal{T}}^F & \Sigma_{\mathcal{F}\mathcal{F}}^F & 0 & 0 & C_{\Gamma} \\ \hline 0 & 0 & 0 & 0 & -E_{\mathcal{T}} & -E_{\mathcal{F}} \\ 0 & 0 & 0 & E_{\mathcal{T}}^\dagger & \Sigma_{\mathcal{T}\mathcal{T}}^S & \Sigma_{\mathcal{T}\mathcal{F}}^S \\ 0 & 0 & 0 & E_{\mathcal{F}}^\dagger & \Sigma_{\mathcal{F}\mathcal{T}}^S & \Sigma_{\mathcal{F}\mathcal{F}}^S \end{array} \right] \left[\begin{array}{c} \mathbf{V}_{\mathcal{T}^F} \\ \mathbf{P}_{\mathcal{T}^F} \\ \mathbf{P}_{\mathcal{F}^F} \\ \hline \mathbf{S}_{\mathcal{T}^S} \\ \mathbf{V}_{\mathcal{T}^S}^S \\ \mathbf{V}_{\mathcal{F}^S}^S \end{array} \right] = \left[\begin{array}{c} 0 \\ G_{\mathcal{T}^F} \\ 0 \\ \hline 0 \\ 0 \\ F_{\mathcal{T}^S} \\ 0 \end{array} \right]$$

- Rearrangement of the dofs: first the cell unknowns and then the face unknowns

$$\left[\begin{array}{cc|cc|c} \mathbf{M}_{\mathcal{T}\mathcal{T}}^{v^F} & 0 & 0 & 0 & 0 \\ 0 & \mathbf{M}_{\mathcal{T}\mathcal{T}}^F & 0 & 0 & 0 \\ 0 & 0 & \mathbf{M}_{\mathcal{T}\mathcal{T}}^\epsilon & 0 & 0 \\ 0 & 0 & 0 & \mathbf{M}_{\mathcal{T}\mathcal{T}}^S & 0 \\ 0 & 0 & 0 & 0 & 0 \\ 0 & 0 & 0 & 0 & 0 \end{array} \right] \frac{d}{dt} \left[\begin{array}{c} \mathbf{V}_{\mathcal{T}^F} \\ \mathbf{P}_{\mathcal{T}^F} \\ \mathbf{S}_{\mathcal{T}^S} \\ \mathbf{V}_{\mathcal{T}^S}^S \\ \mathbf{P}_{\mathcal{F}^F} \\ \mathbf{V}_{\mathcal{F}^S}^S \end{array} \right] + \left[\begin{array}{ccc|ccc} 0 & -G_{\mathcal{T}} & 0 & 0 & -G_{\mathcal{F}} & 0 \\ G_{\mathcal{T}}^\dagger & \Sigma_{\mathcal{T}\mathcal{T}}^F & 0 & 0 & \Sigma_{\mathcal{T}\mathcal{F}}^F & 0 \\ 0 & 0 & 0 & -E_{\mathcal{T}} & 0 & -E_{\mathcal{F}} \\ 0 & 0 & E_{\mathcal{T}}^\dagger & \Sigma_{\mathcal{T}\mathcal{T}}^S & 0 & \Sigma_{\mathcal{T}\mathcal{F}}^S \\ \hline G_{\mathcal{F}}^\dagger & \Sigma_{\mathcal{F}\mathcal{T}}^F & 0 & 0 & \Sigma_{\mathcal{F}\mathcal{F}}^F & C^{\Gamma} \\ 0 & 0 & E_{\mathcal{F}}^\dagger & \Sigma_{\mathcal{F}\mathcal{T}}^S & -C^{\Gamma} & \Sigma_{\mathcal{F}\mathcal{F}}^S \end{array} \right] \left[\begin{array}{c} \mathbf{V}_{\mathcal{T}^F} \\ \mathbf{P}_{\mathcal{T}^F} \\ \mathbf{S}_{\mathcal{T}^S} \\ \mathbf{V}_{\mathcal{T}^S}^S \\ \mathbf{P}_{\mathcal{F}^F} \\ \mathbf{V}_{\mathcal{F}^S}^S \end{array} \right] = \left[\begin{array}{c} 0 \\ G_{\mathcal{T}^F} \\ 0 \\ \hline 0 \\ 0 \\ F_{\mathcal{T}^S} \\ 0 \end{array} \right]$$

SDIRK($s, s + 1$) schemes

- Let us consider the following ODE, with $t \in J$ and $f : \mathbb{R} \times \mathbb{R}^m \rightarrow \mathbb{R}^m$,

$$\begin{cases} y'(t) = f(t, y(t)), & \forall t \in J, \\ y|_{t=0} = y_0 \in \mathbb{R}^m, \end{cases}$$

- SDIRK($s, s + 1$) consist in solving sequentially for all $1 \leq i \leq s$,

$$\left\{ \begin{array}{l} u_{\textcolor{red}{i}}^{[n]} = u_{n-1} + \Delta t \sum_{j=1}^{\textcolor{red}{i}} a_{ij} f(t_{n-1} + c_j \Delta t, u_j^{[n]}) \\ u_n = u_{n-1} + \Delta t \sum_{j=1}^s b_j f(t_{n-1} + c_j \Delta t, u_j^{[n]}) \end{array} \right. \quad \text{with} \quad \begin{array}{c|ccccc} c_1 & a_* & 0 & \cdots & 0 \\ c_2 & a_{21} & a_* & \ddots & 0 \\ \vdots & \vdots & \ddots & \ddots & \vdots \\ c_s & a_{s1} & \cdots & a_{s,s-1} & a_* \\ \hline b_1 & & \cdots & b_{s-1} & b_s \end{array}$$

SDIRK($s, s+1$) schemes

- Let us consider the following ODE, with $t \in J$ and $f : \mathbb{R} \times \mathbb{R}^m \rightarrow \mathbb{R}^m$,

$$\begin{cases} y'(t) = f(t, y(t)), & \forall t \in J, \\ y|_{t=0} = y_0 \in \mathbb{R}^m, \end{cases}$$

- SDIRK($s, s+1$) consist in solving sequentially for all $1 \leq i \leq s$,

$$\begin{cases} u_{\textcolor{red}{i}}^{[n]} = u_{n-1} + \Delta t \sum_{j=1}^{\textcolor{red}{i}} a_{ij} f(t_{n-1} + c_j \Delta t, u_j^{[n]}) \\ u_n = u_{n-1} + \Delta t \sum_{j=1}^s b_j f(t_{n-1} + c_j \Delta t, u_j^{[n]}) \end{cases} \quad \text{with}$$

c_1	a_*	0	\cdots	0
c_2	a_{21}	a_*	\ddots	0
\vdots	\vdots	\ddots	\ddots	\vdots
c_s	a_{s1}	\cdots	$a_{s,s-1}$	a_*
	b_1	\cdots	b_{s-1}	b_s

SDIRK($s, s+1$) Butcher tableaux for $s \in \{1, 2, 3\}$

$$\begin{array}{c|c} 1/2 & 1/2 \\ \hline & 1 \end{array}$$

(a) SDIRK(1, 2)

$$\begin{array}{c|cc} 1/4 & 1/4 & 0 \\ \hline 3/4 & 1/2 & 1/4 \\ & 1/2 & 1/2 \end{array}$$

(b) SDIRK(2, 3)

$$\begin{array}{c|ccc} \gamma & \gamma & 0 & 0 \\ \hline 1/2 & 1/2 - \gamma & \gamma & 0 \\ 1 - \gamma & 2\gamma & 1 - 4\gamma & \gamma \\ \hline \delta & 1 - 2\delta & \delta & \delta \end{array}$$

(c) SDIRK(3,4)

Tab. 1: Butcher tableaux corresponding for some SDIRK($s, s+1$) schemes studied

SDIRK-HHO scheme

- Face-based sparse linear system to be solved at each stage.

- We solve sequentially for all $1 \leq i \leq s$,

$$\left[\begin{array}{c|cc|cc} \mathbf{M}_{\mathcal{T}\mathcal{T}}^{v^F} & 0 & 0 & 0 & 0 \\ \hline 0 & \mathbf{M}_{\mathcal{T}\mathcal{T}}^F & 0 & 0 & 0 \\ \hline 0 & 0 & \mathbf{M}_{\mathcal{T}\mathcal{T}}^e & 0 & 0 \\ \hline 0 & 0 & 0 & \mathbf{M}_{\mathcal{T}\mathcal{T}}^s & 0 & 0 \\ \hline 0 & 0 & 0 & 0 & 0 & 0 \\ \hline 0 & 0 & 0 & 0 & 0 & 0 \end{array} \right] \left[\begin{array}{c} \mathbf{V}_{\mathcal{T}^F}^{F,n,i} \\ \mathbf{P}_{\mathcal{T}^F}^{F,n,i} \\ \mathbf{S}_{\mathcal{T}^s}^{s,n,i} \\ \mathbf{V}_{\mathcal{T}^s}^{s,n,i} \\ \mathbf{P}_{\mathcal{F}^F}^{F,n,i} \\ \mathbf{V}_{\mathcal{F}^s}^{s,n,i} \end{array} \right] = \left[\begin{array}{c|cc|cc|cc} \mathbf{M}_{\mathcal{T}\mathcal{T}}^{v^F} & 0 & 0 & 0 & 0 & 0 & 0 \\ \hline 0 & \mathbf{M}_{\mathcal{T}\mathcal{T}}^F & 0 & 0 & 0 & 0 & 0 \\ \hline 0 & 0 & \mathbf{M}_{\mathcal{T}\mathcal{T}}^e & 0 & 0 & 0 & 0 \\ \hline 0 & 0 & 0 & \mathbf{M}_{\mathcal{T}\mathcal{T}}^s & 0 & 0 & 0 \\ \hline 0 & 0 & 0 & 0 & 0 & 0 & 0 \\ \hline 0 & 0 & 0 & 0 & 0 & 0 & 0 \end{array} \right] \left[\begin{array}{c} \mathbf{V}_{\mathcal{T}^F}^{F,n-1} \\ \mathbf{P}_{\mathcal{T}^F}^{F,n-1} \\ \mathbf{S}_{\mathcal{T}^s}^{s,n-1} \\ \mathbf{V}_{\mathcal{T}^s}^{s,n-1} \\ \mathbf{P}_{\mathcal{F}^F}^{F,n-1} \\ \mathbf{V}_{\mathcal{F}^s}^{s,n-1} \end{array} \right]$$

$$+ \Delta t \sum_{j=1}^i a_{ij} \left(\left[\begin{array}{c} 0 \\ G_{\mathcal{T}^F}^{n-1+c_j} \\ 0 \\ F_{\mathcal{T}^s}^{n-1+c_j} \\ 0 \\ 0 \end{array} \right] - \left[\begin{array}{c|cc|cc|cc} 0 & -G_{\mathcal{T}} & 0 & 0 & -G_{\mathcal{F}} & 0 & 0 \\ \hline G_{\mathcal{T}}^\dagger & \Sigma_{\mathcal{T}\mathcal{T}}^F & 0 & 0 & \Sigma_{\mathcal{T}\mathcal{F}}^F & 0 & 0 \\ \hline 0 & 0 & 0 & -E_{\mathcal{T}} & 0 & -E_{\mathcal{F}} & 0 \\ \hline 0 & 0 & E_{\mathcal{T}}^\dagger & \Sigma_{\mathcal{T}\mathcal{T}}^s & 0 & \Sigma_{\mathcal{T}\mathcal{F}}^s & 0 \\ \hline G_{\mathcal{F}}^\dagger & \Sigma_{\mathcal{F}\mathcal{T}}^F & 0 & 0 & \Sigma_{\mathcal{F}\mathcal{F}}^F & C^F & 0 \\ \hline 0 & 0 & E_{\mathcal{F}}^\dagger & \Sigma_{\mathcal{F}\mathcal{T}}^s & -C^F & \Sigma_{\mathcal{F}\mathcal{F}}^s & 0 \end{array} \right] \left[\begin{array}{c} \mathbf{V}_{\mathcal{T}^F}^{F,n,j} \\ \mathbf{P}_{\mathcal{T}^F}^{F,n,j} \\ \mathbf{S}_{\mathcal{T}^s}^{s,n,j} \\ \mathbf{V}_{\mathcal{T}^s}^{s,n,j} \\ \mathbf{P}_{\mathcal{F}^F}^{F,n,j} \\ \mathbf{V}_{\mathcal{F}^s}^{s,n,j} \end{array} \right] \right)$$

SDIRK-HHO scheme

■ Face-based sparse linear system to be solved at each stage.

■ We solve sequentially for all $1 \leq i \leq s$,

$$\begin{bmatrix} \mathbf{M}_{TT}^{v^F} & 0 & 0 & 0 & 0 \\ 0 & \mathbf{M}_{TT}^F & 0 & 0 & 0 \\ 0 & 0 & \mathbf{M}_{TT}^e & 0 & 0 \\ 0 & 0 & 0 & \mathbf{M}_{TT}^S & 0 \\ 0 & 0 & 0 & 0 & 0 \\ 0 & 0 & 0 & 0 & 0 \end{bmatrix} \begin{bmatrix} \mathbf{V}_{T^F}^{n,i} \\ \mathbf{P}_{T^F}^{n,i} \\ \mathbf{S}_{T^S}^{n,i} \\ \mathbf{V}_{T^S}^{n,i} \\ \mathbf{P}_{\mathcal{F}^F}^{n,i} \\ \mathbf{V}_{\mathcal{F}^S}^{n,i} \end{bmatrix} = \begin{bmatrix} \mathbf{M}_{TT}^{v^F} & 0 & 0 & 0 & 0 \\ 0 & \mathbf{M}_{TT}^F & 0 & 0 & 0 \\ 0 & 0 & \mathbf{M}_{TT}^e & 0 & 0 \\ 0 & 0 & 0 & \mathbf{M}_{TT}^S & 0 \\ 0 & 0 & 0 & 0 & 0 \\ 0 & 0 & 0 & 0 & 0 \end{bmatrix} \begin{bmatrix} \mathbf{V}_{T^F}^{n-1} \\ \mathbf{P}_{T^F}^{n-1} \\ \mathbf{S}_{T^S}^{n-1} \\ \mathbf{V}_{T^S}^{n-1} \\ \mathbf{P}_{\mathcal{F}^F}^{n-1} \\ \mathbf{V}_{\mathcal{F}^S}^{n-1} \end{bmatrix}$$

$$+ \Delta t \sum_{j=1}^i a_{ij} \begin{pmatrix} 0 \\ \mathbf{G}_{T^F}^{n-1+c_j} \\ 0 \\ \mathbf{F}_{T^S}^{n-1+c_j} \\ 0 \\ 0 \end{pmatrix} - \begin{bmatrix} 0 & -\mathbf{G}_T & 0 & 0 & -\mathbf{G}_{\mathcal{F}} & 0 \\ \mathbf{G}_T^\dagger & \Sigma_{TT}^F & 0 & 0 & \Sigma_{T\mathcal{F}}^F & 0 \\ 0 & 0 & 0 & -\mathbf{E}_T & 0 & -\mathbf{E}_{\mathcal{F}} \\ 0 & 0 & \mathbf{E}_T^\dagger & \Sigma_{TT}^S & 0 & \Sigma_{T\mathcal{F}}^S \\ \mathbf{G}_{\mathcal{F}}^\dagger & \Sigma_{\mathcal{F}T}^F & 0 & 0 & \Sigma_{\mathcal{F}\mathcal{F}}^F & \mathbf{C}^\Gamma \\ 0 & 0 & \mathbf{E}_{\mathcal{F}}^\dagger & \Sigma_{\mathcal{F}T}^S & -\mathbf{C}^\Gamma & \Sigma_{\mathcal{F}\mathcal{F}}^S \end{bmatrix} \begin{bmatrix} \mathbf{V}_{T^F}^{n,j} \\ \mathbf{P}_{T^F}^{n,j} \\ \mathbf{S}_{T^S}^{n,j} \\ \mathbf{V}_{T^S}^{n,j} \\ \mathbf{P}_{\mathcal{F}^F}^{n,j} \\ \mathbf{V}_{\mathcal{F}^S}^{n,j} \end{bmatrix}$$

■ The upper 4×4 submatrix associated with the acoustic and elastic cell unknowns is block-diagonal.

► Schur complement procedure

ERK(s) schemes

- ERK(s) consist in updating sequentially for all $1 \leq i \leq s$,

$$\begin{cases} u_i^{[n]} = u_{n-1} + \Delta t \sum_{j=1}^{\textcolor{red}{i-1}} a_{ij} f(t_{n-1} + c_j \Delta t, u_j^{[n]}) \\ u_n = u_{n-1} + \Delta t \sum_{j=1}^s b_j f\left(t_{n-1} + c_j \Delta t, U_j^{[n]}\right) \end{cases}$$

with

$$\frac{\begin{array}{c|ccccc} c_1 & 0 & \cdots & \cdots & 0 \\ c_2 & a_{21} & 0 & \cdots & 0 \\ \vdots & \vdots & \ddots & \ddots & \vdots \\ c_s & a_{s1} & \cdots & a_{s,s-1} & 0 \end{array}}{\begin{array}{ccccc} b_1 & \cdots & b_{s-1} & b_s \end{array}}$$

ERK(s) schemes

- ERK(s) consist in updating sequentially for all $1 \leq i \leq s$,

$$\begin{cases} u_i^{[n]} = u_{n-1} + \Delta t \sum_{j=1}^{\textcolor{red}{i-1}} a_{ij} f(t_{n-1} + c_j \Delta t, u_j^{[n]}) \\ u_n = u_{n-1} + \Delta t \sum_{j=1}^s b_j f\left(t_{n-1} + c_j \Delta t, U_j^{[n]}\right) \end{cases}$$

with

$$\begin{array}{c|ccccc} c_1 & 0 & \cdots & \cdots & 0 \\ c_2 & a_{21} & 0 & \cdots & 0 \\ \vdots & \vdots & \ddots & \ddots & \vdots \\ c_s & a_{s1} & \cdots & a_{s,s-1} & 0 \\ \hline b_1 & \cdots & b_{s-1} & b_s \end{array}$$

ERK(s) Butcher tableaux for $s \in \{1, 2, 3, 4\}$

$$\begin{array}{c|c} 0 & 0 \\ \hline 1 \end{array}$$

(a) ERK(1): forward Euler

$$\begin{array}{c|cc} 0 & 0 & 0 \\ 1/2 & 1/2 & 0 \\ \hline 0 & 1 \end{array}$$

(b) ERK(2): explicit midpoint

$$\begin{array}{c|ccc} 0 & 0 & 0 & 0 \\ 1/2 & 1/2 & 0 & 0 \\ 1 & -1 & 2 & 0 \\ \hline 1/6 & 2/3 & 1/6 \end{array}$$

(c) ERK(3)

$$\begin{array}{c|ccccc} 0 & 0 & 0 & 0 & 0 \\ 1/2 & 1/2 & 0 & 0 & 0 \\ 1/2 & 0 & 1/2 & 0 & 0 \\ 1 & 0 & 0 & 1 & 0 \\ \hline 1/6 & 1/3 & 1/3 & 1/6 \end{array}$$

(d) ERK(4)

Tab. 2: Butcher tableaux corresponding of the ERK(s) schemes studied

HHO-ERK scheme

- ERK-HHO is not fully explicit

- ▶ Implicit coupling of face unknowns is hidden in ERK schemes

$$\left[\begin{array}{c|cc|cc} \mathbf{M}_{\mathcal{T}\mathcal{T}}^{v^F} & 0 & 0 & 0 & 0 \\ \hline 0 & \mathbf{M}_{\mathcal{T}\mathcal{T}}^F & 0 & 0 & 0 \\ \hline 0 & 0 & \mathbf{M}_{\mathcal{T}\mathcal{T}}^e & 0 & 0 \\ \hline 0 & 0 & 0 & \mathbf{M}_{\mathcal{T}\mathcal{T}}^s & 0 & 0 \\ \hline 0 & 0 & 0 & 0 & 0 & 0 \\ \hline 0 & 0 & 0 & 0 & 0 & 0 \end{array} \right] \left[\begin{array}{c} \mathbf{V}_{\mathcal{T}^F}^{n,i} \\ \mathbf{P}_{\mathcal{T}^F}^{n,i} \\ \mathbf{S}_{\mathcal{T}^s}^{n,i} \\ \mathbf{V}_{\mathcal{T}^s}^{n,i} \\ \mathbf{P}_{\mathcal{F}^F}^{n,i} \\ \mathbf{V}_{\mathcal{F}^s}^{n,i} \end{array} \right] = \left[\begin{array}{c|cc|cc|c} \mathbf{M}_{\mathcal{T}\mathcal{T}}^{v^F} & 0 & 0 & 0 & 0 & \mathbf{V}_{\mathcal{T}^F}^{n-1} \\ \hline 0 & \mathbf{M}_{\mathcal{T}\mathcal{T}}^F & 0 & 0 & 0 & \mathbf{P}_{\mathcal{T}^F}^{n-1} \\ \hline 0 & 0 & \mathbf{M}_{\mathcal{T}\mathcal{T}}^e & 0 & 0 & \mathbf{S}_{\mathcal{T}^s}^{n-1} \\ \hline 0 & 0 & 0 & \mathbf{M}_{\mathcal{T}\mathcal{T}}^s & 0 & \mathbf{V}_{\mathcal{T}^s}^{n-1} \\ \hline 0 & 0 & 0 & 0 & 0 & \mathbf{P}_{\mathcal{F}^F}^{n-1} \\ \hline 0 & 0 & 0 & 0 & 0 & \mathbf{V}_{\mathcal{F}^s}^{n-1} \end{array} \right]$$

$$+ \Delta t \sum_{j=1}^{i-1} a_{ij} \left(\begin{bmatrix} 0 \\ G_{\mathcal{T}^F}^{n-1+c_j} \\ \hline 0 \\ F_{\mathcal{T}^s}^{n-1+c_j} \\ \hline 0 \\ 0 \end{bmatrix} - \begin{bmatrix} 0 & -G_{\mathcal{T}} & 0 & 0 & -G_{\mathcal{F}} & 0 \\ G_{\mathcal{T}}^\dagger & \Sigma_{\mathcal{T}\mathcal{T}}^F & 0 & 0 & \Sigma_{\mathcal{T}\mathcal{F}}^F & 0 \\ \hline 0 & 0 & 0 & -E_{\mathcal{T}} & 0 & -E_{\mathcal{F}} \\ 0 & 0 & E_{\mathcal{T}}^\dagger & \Sigma_{\mathcal{T}\mathcal{T}}^s & 0 & \Sigma_{\mathcal{T}\mathcal{F}}^s \\ \hline G_{\mathcal{F}}^\dagger & \Sigma_{\mathcal{F}\mathcal{T}}^F & 0 & 0 & \Sigma_{\mathcal{F}\mathcal{F}}^F & C^\Gamma \\ 0 & 0 & E_{\mathcal{F}}^\dagger & \Sigma_{\mathcal{F}\mathcal{T}}^s & -C^\Gamma & \Sigma_{\mathcal{F}\mathcal{F}}^s \end{bmatrix} \begin{bmatrix} \mathbf{V}_{\mathcal{T}^F}^{n,j} \\ \mathbf{P}_{\mathcal{T}^F}^{n,j} \\ \mathbf{S}_{\mathcal{T}^s}^{n,j} \\ \mathbf{V}_{\mathcal{T}^s}^{n,j} \\ \mathbf{P}_{\mathcal{F}^F}^{n,j} \\ \mathbf{V}_{\mathcal{F}^s}^{n,j} \end{bmatrix} \right)$$

HHO-ERK scheme

- ERK-HHO is not fully explicit

► Implicit coupling of face unknowns is hidden in ERK schemes

$$\begin{bmatrix} \mathbf{M}_{\mathcal{T}\mathcal{T}}^{v^F} & 0 & | & 0 & 0 & | & 0 & 0 \\ 0 & \mathbf{M}_{\mathcal{T}\mathcal{T}}^F & | & 0 & 0 & | & 0 & 0 \\ \hline 0 & 0 & | & \mathbf{M}_{\mathcal{T}\mathcal{T}}^e & 0 & | & 0 & 0 \\ 0 & 0 & | & 0 & \mathbf{M}_{\mathcal{T}\mathcal{T}}^S & | & 0 & 0 \\ \hline 0 & 0 & | & 0 & 0 & | & 0 & 0 \\ 0 & 0 & | & 0 & 0 & | & 0 & 0 \end{bmatrix} = \begin{bmatrix} \mathbf{M}_{\mathcal{T}\mathcal{T}}^{v^F} & 0 & | & \mathbf{V}_{\mathcal{T}^F}^{n,i} & & | & \mathbf{M}_{\mathcal{T}\mathcal{T}}^{v^F} & 0 & | & 0 & 0 & | & 0 & 0 \\ P_{\mathcal{T}^F}^{n,i} & & | & & & | & 0 & \mathbf{M}_{\mathcal{T}\mathcal{T}}^F & | & 0 & 0 & | & 0 & 0 \\ S_{\mathcal{T}^S}^{n,i} & & | & & & | & 0 & 0 & | & \mathbf{M}_{\mathcal{T}\mathcal{T}}^e & 0 & | & 0 & 0 \\ V_{\mathcal{T}^S}^{n,i} & & | & & & | & 0 & 0 & | & 0 & \mathbf{M}_{\mathcal{T}\mathcal{T}}^S & | & 0 & 0 \\ \hline P_{\mathcal{F}^F}^{n,i} & & | & & & | & 0 & 0 & | & 0 & 0 & | & 0 & 0 \\ V_{\mathcal{F}^S}^{n,i} & & | & & & | & 0 & 0 & | & 0 & 0 & | & 0 & 0 \end{bmatrix}$$

$$+ \Delta t \sum_{j=1}^{i-1} a_{ij} \begin{pmatrix} 0 \\ G_{\mathcal{T}^F}^{n-1+c_j} \\ \hline 0 \\ F_{\mathcal{T}^S}^{n-1+c_j} \\ \hline 0 \\ 0 \end{pmatrix} - \begin{bmatrix} 0 & -G_{\mathcal{T}} & 0 & 0 & -G_{\mathcal{F}} & 0 \\ G_{\mathcal{T}}^\dagger & \Sigma_{\mathcal{T}\mathcal{T}}^F & 0 & 0 & \Sigma_{\mathcal{T}\mathcal{F}}^F & 0 \\ \hline 0 & 0 & 0 & -E_{\mathcal{T}} & 0 & -E_{\mathcal{F}} \\ 0 & 0 & E_{\mathcal{T}}^\dagger & \Sigma_{\mathcal{T}\mathcal{T}}^S & 0 & \Sigma_{\mathcal{T}\mathcal{F}}^S \\ \hline G_{\mathcal{F}}^\dagger & \Sigma_{\mathcal{F}\mathcal{T}}^F & 0 & 0 & \Sigma_{\mathcal{F}\mathcal{F}}^F & C^{\Gamma} \\ 0 & 0 & E_{\mathcal{F}}^\dagger & \Sigma_{\mathcal{F}\mathcal{T}}^S & -C^{\Gamma} & \Sigma_{\mathcal{F}\mathcal{F}}^S \end{bmatrix} \begin{bmatrix} \mathbf{V}_{\mathcal{T}^F}^{n,j} \\ P_{\mathcal{T}^F}^{n,j} \\ S_{\mathcal{T}^S}^{n,j} \\ V_{\mathcal{T}^S}^{n,j} \\ \hline P_{\mathcal{F}^F}^{n,j} \\ V_{\mathcal{F}^S}^{n,j} \end{bmatrix}$$

- Fortunately, $\begin{bmatrix} \Sigma_{\mathcal{F}\mathcal{F}}^F & C^{\Gamma} \\ -C^{\Gamma} & \Sigma_{\mathcal{F}\mathcal{F}}^S \end{bmatrix}$ has a block diagonal structure for a **mixed-order** discretization

Rearrangement of the face terms for the inversion of coupling block

- Distinguish between internal faces and interfaces
- Uncover a block diagonal structure

$$\begin{array}{c|cc}
 \left[\begin{array}{cc|cc} \Sigma_{\mathcal{F}\mathcal{F}}^F & 0 & 0 & 0 \\ 0 & \Sigma_{\mathcal{F}\mathcal{F}}^S & 0 & 0 \\ \hline 0 & 0 & \Sigma_{\mathcal{F}\mathcal{F}}^F & C_F^\dagger \\ 0 & 0 & -C_F & \Sigma_{\mathcal{F}\mathcal{F}}^S \end{array} \right] & \left[\begin{array}{c} P_{\mathcal{F}_h^{OF}} \\ V_{\mathcal{F}_h^{OS}}^S \end{array} \right] \\
 \hline
 \left[\begin{array}{cc|cc} \Sigma_{F1}^F & C_{F1}^\dagger & 0 & 0 \\ -C_{F1} & \Sigma_{F1}^S & 0 & 0 \\ \hline 0 & 0 & \ddots & 0 \\ 0 & 0 & \ddots & 0 \\ \hline 0 & 0 & 0 & \Sigma_{Fn}^F \\ 0 & 0 & 0 & -C_{Fn} \end{array} \right] & \left[\begin{array}{c} P_{F1} \\ V_{F1}^S \\ \vdots \\ \vdots \\ P_{Fn} \\ V_{Fn}^S \end{array} \right]
 \end{array}$$

Rearrangement of the face terms for the inversion of coupling block

- Distinguish between internal faces and interfaces
- Uncover a block diagonal structure

$$\begin{array}{c}
 \left[\begin{array}{cc|cc} \Sigma_{\mathcal{F}\mathcal{F}}^F & 0 & 0 & 0 \\ 0 & \Sigma_{\mathcal{F}\mathcal{F}}^S & 0 & 0 \\ \hline 0 & 0 & \Sigma_{\mathcal{F}\mathcal{F}}^F & C_\Gamma^\dagger \\ 0 & 0 & -C_\Gamma & \Sigma_{\mathcal{F}\mathcal{F}}^S \end{array} \right] \left[\begin{array}{c} P_{\mathcal{F}^{\circ F}_h} \\ V_{\mathcal{F}^{\circ S}_h}^S \end{array} \right] \\
 \xrightarrow{\text{dashed arrow}}
 \left[\begin{array}{cc|cc|cc} \Sigma_{F^1}^F & C_{F^1}^\dagger & 0 & 0 & 0 & 0 \\ -C_{F^1} & \Sigma_{F^1}^S & 0 & 0 & 0 & 0 \\ \hline 0 & 0 & \ddots & & 0 & 0 \\ 0 & 0 & & \ddots & 0 & 0 \\ 0 & 0 & 0 & 0 & \Sigma_{F^n}^F & C_{F^n}^\dagger \\ 0 & 0 & 0 & 0 & -C_{F^n} & \Sigma_{F^n}^S \end{array} \right] \left[\begin{array}{c} P_{F^1} \\ V_{F^1}^S \\ \vdots \\ \vdots \\ P_{F^n} \\ V_{F^n}^S \end{array} \right]
 \end{array}$$

1st step of the ERK-HHO scheme

- 1st step:** $(V_{\mathcal{T}^F}^{n,1}, P_{\mathcal{T}^F}^{n,1}, S_{\mathcal{T}^S}^{n,1}, V_{\mathcal{T}^S}^{n,1}) := (V_{\mathcal{T}^F}^{n-1}, P_{\mathcal{T}^F}^{n-1}, S_{\mathcal{T}^S}^{n-1}, V_{\mathcal{T}^S}^{n-1})$ and solve

$$\left[\begin{array}{cc} \Sigma_{\mathcal{F}\mathcal{F}}^F & C_\Gamma^\dagger \\ -C_\Gamma & \Sigma_{\mathcal{F}\mathcal{F}}^S \end{array} \right] \left[\begin{array}{c} P_{\mathcal{F}^F}^{n,1} \\ V_{\mathcal{F}^S}^{n,1} \end{array} \right] = - \left(\left[\begin{array}{cc} G_\mathcal{F}^\dagger & \Sigma_{\mathcal{F}\mathcal{T}}^F \end{array} \right] \left[\begin{array}{c} V_{\mathcal{T}^F}^{n,1} \\ P_{\mathcal{T}^F}^{n,1} \end{array} \right] + \left[\begin{array}{cc} E_\mathcal{F}^\dagger & \Sigma_{\mathcal{F}\mathcal{T}}^S \end{array} \right] \left[\begin{array}{c} S_{\mathcal{T}^S}^{n,1} \\ V_{\mathcal{T}^S}^{n,1} \end{array} \right] \right)$$

2nd step: ERK-HHO scheme

- 2nd step: If $s \geq 2$, solve sequentially for all $2 \leq i \leq s$,

$$\rightarrow \begin{bmatrix} \mathbf{M}_{\mathcal{T}\mathcal{T}}^{v^p} & 0 & 0 & 0 \\ 0 & \mathbf{M}_{\mathcal{T}\mathcal{T}}^F & 0 & 0 \\ 0 & 0 & \mathbf{M}_{\mathcal{T}\mathcal{T}}^\epsilon & 0 \\ 0 & 0 & 0 & \mathbf{M}_{\mathcal{T}\mathcal{T}}^S \end{bmatrix} \begin{bmatrix} \mathbf{V}_{\mathcal{T}^p}^{v^p n,i} \\ \mathbf{P}_{\mathcal{T}^p}^{v^p n,i} \\ \mathbf{S}_{\mathcal{T}^s}^{n,i} \\ \mathbf{V}_{\mathcal{T}^s}^{S n,i} \end{bmatrix} = \begin{bmatrix} \mathbf{M}_{\mathcal{T}\mathcal{T}}^{v^p} & 0 & 0 & 0 \\ 0 & \mathbf{M}_{\mathcal{T}\mathcal{T}}^F & 0 & 0 \\ 0 & 0 & \mathbf{M}_{\mathcal{T}\mathcal{T}}^\epsilon & 0 \\ 0 & 0 & 0 & \mathbf{M}_{\mathcal{T}\mathcal{T}}^S \end{bmatrix} \begin{bmatrix} \mathbf{V}_{\mathcal{T}^p}^{v^p n-1} \\ \mathbf{P}_{\mathcal{T}^p}^{v^p n-1} \\ \mathbf{S}_{\mathcal{T}^s}^{n-1} \\ \mathbf{V}_{\mathcal{T}^s}^{S n-1} \end{bmatrix}$$

$$+ \Delta t \sum_{j=1}^{i-1} a_{ij} \left(\begin{bmatrix} 0 \\ G_{\mathcal{T}^p}^{n-1+c_j} \\ \vdots \\ 0 \\ F_{\mathcal{T}^s}^{n-1+c_j} \end{bmatrix} - \begin{bmatrix} 0 & -G_{\mathcal{T}} & 0 & 0 & -G_{\mathcal{F}} & 0 \\ G_{\mathcal{T}}^\dagger & \Sigma_{\mathcal{T}\mathcal{T}}^F & 0 & 0 & \Sigma_{\mathcal{T}\mathcal{F}}^F & 0 \\ 0 & 0 & 0 & -E_{\mathcal{T}} & 0 & -E_{\mathcal{F}} \\ 0 & 0 & E_{\mathcal{T}}^\dagger & \Sigma_{\mathcal{T}\mathcal{T}}^S & 0 & \Sigma_{\mathcal{T}\mathcal{F}}^S \end{bmatrix} \begin{bmatrix} \mathbf{V}_{\mathcal{T}^p}^{v^p n,j} \\ \mathbf{P}_{\mathcal{T}^p}^{v^p n,j} \\ \mathbf{S}_{\mathcal{T}^s}^{n,j} \\ \mathbf{V}_{\mathcal{T}^s}^{S n,j} \\ \mathbf{P}_{\mathcal{F}^p}^{n,j} \\ \mathbf{V}_{\mathcal{F}^s}^{S n,j} \end{bmatrix} \right)$$

2nd step: ERK-HHO scheme

- 2nd step: If $s \geq 2$, solve sequentially for all $2 \leq i \leq s$,

$$\begin{aligned} & \rightarrow \left[\begin{array}{cc|cc} \mathbf{M}_{\mathcal{T}\mathcal{T}}^{v^F} & 0 & 0 & 0 \\ 0 & \mathbf{M}_{\mathcal{T}\mathcal{T}}^F & 0 & 0 \\ \hline 0 & 0 & \mathbf{M}_{\mathcal{T}\mathcal{T}}^\epsilon & 0 \\ 0 & 0 & 0 & \mathbf{M}_{\mathcal{T}\mathcal{T}}^S \end{array} \right] \left[\begin{array}{c} \mathbf{V}_{\mathcal{T}^F}^{v^F, n, i} \\ \mathbf{P}_{\mathcal{T}^F}^{v^F, n, i} \\ \hline \mathbf{S}_{\mathcal{T}^S}^{n, i} \\ \mathbf{V}_{\mathcal{T}^S}^{S, n, i} \end{array} \right] = \left[\begin{array}{cc|cc} \mathbf{M}_{\mathcal{T}\mathcal{T}}^{v^F} & 0 & 0 & 0 \\ 0 & \mathbf{M}_{\mathcal{T}\mathcal{T}}^F & 0 & 0 \\ \hline 0 & 0 & \mathbf{M}_{\mathcal{T}\mathcal{T}}^\epsilon & 0 \\ 0 & 0 & 0 & \mathbf{M}_{\mathcal{T}\mathcal{T}}^S \end{array} \right] \left[\begin{array}{c} \mathbf{V}_{\mathcal{T}^F}^{F, n-1} \\ \mathbf{P}_{\mathcal{T}^F}^{F, n-1} \\ \hline \mathbf{S}_{\mathcal{T}^S}^{n-1} \\ \mathbf{V}_{\mathcal{T}^S}^{S, n-1} \end{array} \right] \\ & + \Delta t \sum_{j=1}^{i-1} a_{ij} \left(\left[\begin{array}{c} 0 \\ \mathbf{G}_{\mathcal{T}^F}^{n-1+c_j} \\ \hline 0 \\ \mathbf{F}_{\mathcal{T}^S}^{n-1+c_j} \end{array} \right] - \left[\begin{array}{cc|cc|cc} 0 & -\mathbf{G}_{\mathcal{T}} & 0 & 0 & -\mathbf{G}_{\mathcal{F}} & 0 \\ \mathbf{G}_{\mathcal{T}}^\dagger & \Sigma_{\mathcal{T}\mathcal{T}}^F & 0 & 0 & \Sigma_{\mathcal{T}\mathcal{F}}^F & 0 \\ \hline 0 & 0 & 0 & -\mathbf{E}_{\mathcal{T}} & 0 & -\mathbf{E}_{\mathcal{F}} \\ 0 & 0 & \mathbf{E}_{\mathcal{T}}^\dagger & \Sigma_{\mathcal{T}\mathcal{T}}^S & 0 & \Sigma_{\mathcal{T}\mathcal{F}}^S \end{array} \right] \left[\begin{array}{c} \mathbf{V}_{\mathcal{T}^F}^{F, n, j} \\ \mathbf{P}_{\mathcal{T}^F}^{F, n, j} \\ \hline \mathbf{S}_{\mathcal{T}^S}^{n, j} \\ \mathbf{V}_{\mathcal{T}^S}^{S, n, j} \\ \mathbf{P}_{\mathcal{F}^F}^{S, n, j} \\ \mathbf{V}_{\mathcal{F}^S}^{S, n, j} \end{array} \right] \right) \\ & \rightarrow \left[\begin{array}{cc} \Sigma_{\mathcal{F}\mathcal{F}}^F & \mathbf{C}_\Gamma^\dagger \\ -\mathbf{C}_\Gamma & \Sigma_{\mathcal{F}\mathcal{F}}^S \end{array} \right] \left[\begin{array}{c} \mathbf{P}_{\mathcal{F}^F}^{F, n, i} \\ \mathbf{V}_{\mathcal{F}^S}^{S, n, i} \end{array} \right] = - \left(\left[\begin{array}{cc} \mathbf{G}_{\mathcal{F}}^\dagger & \Sigma_{\mathcal{F}\mathcal{T}}^F \end{array} \right] \left[\begin{array}{c} \mathbf{V}_{\mathcal{T}^F}^{F, n, i} \\ \mathbf{P}_{\mathcal{T}^F}^{F, n, i} \end{array} \right] + \left[\begin{array}{cc} \mathbf{E}_{\mathcal{F}}^\dagger & \Sigma_{\mathcal{F}\mathcal{T}}^S \end{array} \right] \left[\begin{array}{c} \mathbf{S}_{\mathcal{T}^S}^{n, i} \\ \mathbf{V}_{\mathcal{T}^S}^{S, n, i} \end{array} \right] \right) \end{aligned}$$

Table of Contents

- 1 Motivation
 - Context and issues
 - Introduction to dG and HDG/HHO methods
- 2 Model problem
- 3 RK-HHO discretization
 - HHO space semi-discretization
 - Singly diagonally implicit schemes
 - Explicit schemes
- 4 Numerical results
 - Convergence rates
 - Ricker wavelet
 - Sedimentary basin
- 5 To go further: Unfitted HHO method

Computational parameters

- Space level refinement: $h = 2^{-\ell}$
- Time level refinement: $\Delta t = 0.1 \times 2^{-n}$

Computational parameters

- Space level refinement: $h = 2^{-\ell}$
- Time level refinement: $\Delta t = 0.1 \times 2^{-n}$

Meshes

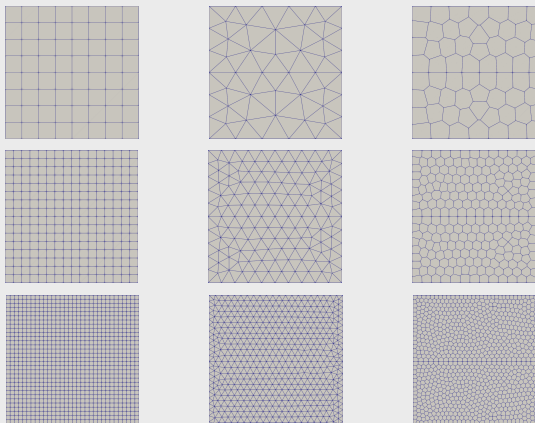


Fig. 9: Cartesian, simplicial and polyhedral meshes for $\ell = \{2, 3, 4\}$

Analytical solution

■ Analytical solution, polynomial in space:

$$\mathbf{u}^{\text{s}}(x, y, t) := \sin(\sqrt{2}\pi t)x^2(1+x)y(1-y) \begin{pmatrix} 1 \\ 1 \end{pmatrix}, \quad u^{\text{f}}(x, y, t) := \sin(\sqrt{2}\pi t)x^2(1-x)y(1-y)$$

Analytical solution

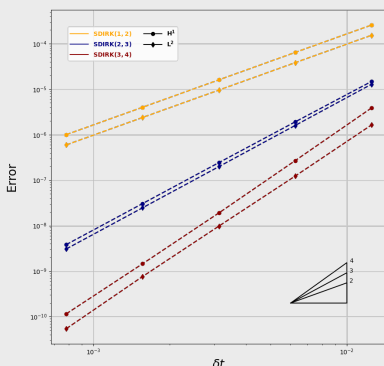
■ Analytical solution, polynomial in space:

$$u^S(x, y, t) := \sin(\sqrt{2}\pi t)x^2(1+x)y(1-y) \begin{pmatrix} 1 \\ 1 \end{pmatrix}, \quad u^F(x, y, t) := \sin(\sqrt{2}\pi t)x^2(1-x)y(1-y)$$

Verification of time convergence rates

► SDIRK-HHO scheme

- $k' = k + 1 = 6$; $\ell = 2$; $n \in \{3, 4, 5, 6, 7\}$
- $\tau_T^F = \mathcal{O}(1)$ and $\tau_T^S = \mathcal{O}(1)$



► ERK-HHO scheme

- $k' = k + 1 = 5$; $\ell = 1$; $n \in \{6, 7, 8, 9\}$
- $\tau_T^F = \mathcal{O}(1)$ and $\tau_T^S = \mathcal{O}(1)$

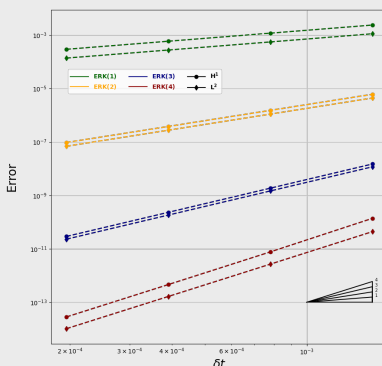


Fig. 10: Errors for the HHO-RK schemes as a function of the time-step.

Analytical solution

■ Analytical solution polynomial in time:

$$\mathbf{u}_S(x, y, t) := xt^2 \sin(\pi x) \sin(\pi y) \begin{pmatrix} 1 \\ 1 \end{pmatrix}, \quad u_F(x, y, t) := xt^2 \sin(\pi x) \sin(\pi y)$$

Analytical solution

■ Analytical solution polynomial in time:

$$u_S(x, y, t) := xt^2 \sin(\pi x) \sin(\pi y) \begin{pmatrix} 1 \\ 1 \end{pmatrix}, \quad u_F(x, y, t) := xt^2 \sin(\pi x) \sin(\pi y)$$

Verification of space convergence rates

► SDIRK(3,4)-HHO scheme

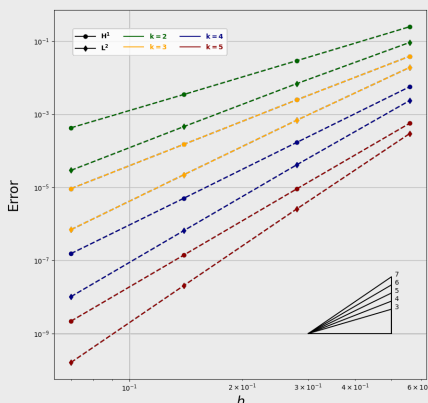
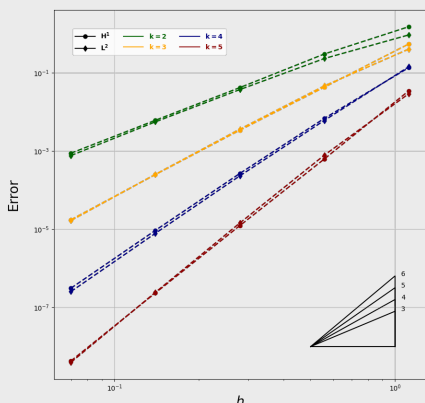
► $n = 8$ ► $\ell \in \{0, 1, 2, 3, 4\}$ 

Fig. 11: Errors for the HHO-SDIRK(3,4) schemes as a function of the mesh-size. **Left pannel:** $\tau_T^F = \mathcal{O}(1)$ and $\tau_T^S = \mathcal{O}(1)$. **Right pannel:** $\tau_T^F = \mathcal{O}(h_T^{-1})$ and $\tau_T^S = \mathcal{O}(h_T^{-1})$

Test case settings

- ▶ **HHO-SDIRK(3,4) scheme**
- ▶ **Computational parameters:** $k = 1$, $\ell = 7$, and $n = 9$
- ▶ **Final simulation time:** $T_f := 1$ s
- ▶ **Homogeneous Dirichlet boundary conditions**
- ▶ **Initial condition:** velocity Ricker wavelet centered at the point $(x_c, y_c) \in \Omega^F$,

$$\mathbf{v}_0(x, y) := \theta \exp\left(-\pi^2 \frac{r^2}{\lambda^2}\right) \begin{pmatrix} x - x_c \\ y - y_c \end{pmatrix}$$

Test case settings

- ▶ **HHO-SDIRK(3,4) scheme**
- ▶ **Computational parameters:** $k = 1$, $\ell = 7$, and $n = 9$
- ▶ **Final simulation time:** $T_f := 1$ s
- ▶ **Homogeneous Dirichlet boundary conditions**
- ▶ **Initial condition:** velocity Ricker wavelet centered at the point $(x_c, y_c) \in \Omega^F$,

$$\mathbf{v}_0(x, y) := \theta \exp\left(-\pi^2 \frac{r^2}{\lambda^2}\right) \begin{pmatrix} x - x_c \\ y - y_c \end{pmatrix}$$

Academic test case:

- ▶ **Homogeneous physical properties:** $\rho^F = \rho^S = 1$, $c_p^F = c_p^S = \sqrt{3}$, $c_s = 1$

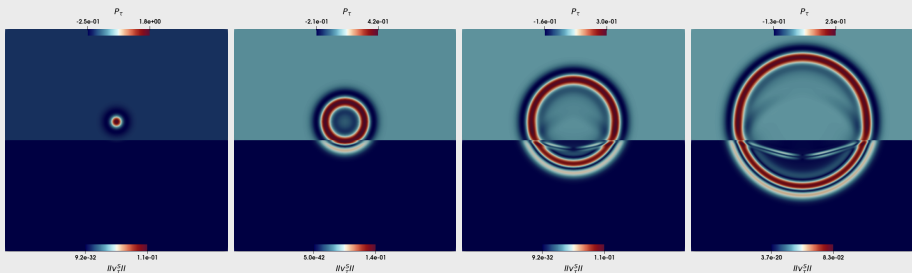


Fig. 12: 2D-Distribution of acoustic pressure (upper side) and elastic velocity norm (lower side) at times $t \in \{0, 0.025, 0.075, 0.15\}$.

Study of the energy of the academic test case

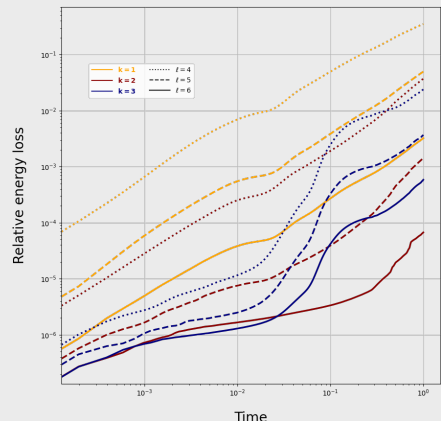
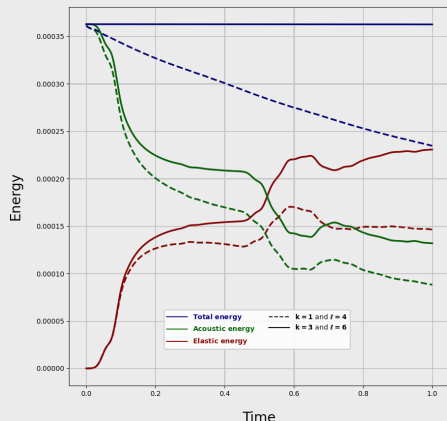


Fig. 13: **Left panel:** Energy repartition as function of the time. **Right panel:** Relative energy loss as function of the time.

Realistic test case with strong property contrast: Granit-Water

■ Physical properties:

- ▶ **Granit:** $\rho^S = 2\,800 \text{ kg.m}^{-3}$, $c_p^S = 5\,000 \text{ m.s}^{-1}$, $c_s = 3\,000 \text{ m.s}^{-1}$
- ▶ **Water:** $\rho^F := 997 \text{ k.m}^{-3}$, $\kappa := 2,1 \times 10^9 \text{ Pa}$, $c_p^F := 1\,450 \text{ m.s}^{-1}$

Realistic test case with strong property contrast: Granit-Water

■ Physical properties:

- ▶ Granit: $\rho^S = 2\,800 \text{ kg.m}^{-3}$, $c_p^S = 5\,000 \text{ m.s}^{-1}$, $c_s = 3\,000 \text{ m.s}^{-1}$
- ▶ Water: $\rho^F := 997 \text{ k.m}^{-3}$, $\kappa := 2,1 \times 10^9 \text{ Pa}$, $c_p^F := 1\,450 \text{ m.s}^{-1}$

■ Computational parameters: ▶ SDIRK(3,4) ▶ $n = 8$

Realistic test case with strong property contrast: Granit-Water

■ Physical properties:

- ▶ **Granit:** $\rho^S = 2\,800 \text{ kg.m}^{-3}$, $c_p^S = 5\,000 \text{ m.s}^{-1}$, $c_s = 3\,000 \text{ m.s}^{-1}$
- ▶ **Water:** $\rho^F := 997 \text{ k.m}^{-3}$, $\kappa := 2,1 \times 10^9 \text{ Pa}$, $c_p^F := 1\,450 \text{ m.s}^{-1}$

■ Computational parameters:

► SDIRK(3,4) ► $n = 8$

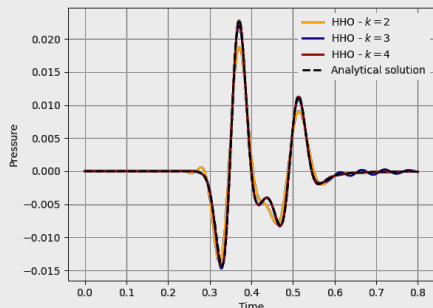
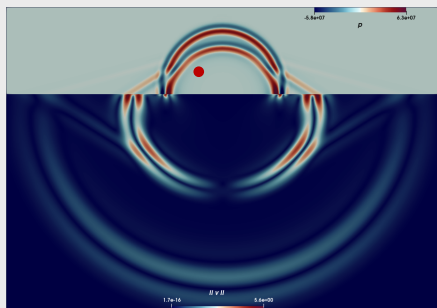


Fig. 14: Left panel: 2D-distribution of acoustic pressure (upper side) and elastic velocity norm (lower side) at time $t = 0.375\text{s}$ for $k = 2$ and $\ell = 7$. Right panel: Comparison of numerical solution on a coarse mesh ($\ell = 5$) to the semi-analytical solution provided by Garfmore.

Propagation of an elastic pulse in a sedimentary basin and atmosphere

■ Physical properties:

- ▶ **Sedimentary basin:** $\rho^s = 1\ 200 \text{ kg.m}^{-3}$, $c_p^s = 3\ 400 \text{ m.s}^{-1}$, $c_s = 1\ 400 \text{ m.s}^{-1}$
- ▶ **Bedrock:** $\rho^s = 5\ 350 \text{ kg.m}^{-3}$, $c_p^s = 3\ 090 \text{ m.s}^{-1}$, $c_s = 2\ 570 \text{ m.s}^{-1}$
- ▶ **Air:** $\rho^F := 1.292 \text{ k.m}^{-3}$, $c_p^F := 340 \text{ m.s}^{-1}$

Propagation of an elastic pulse in a sedimentary basin and atmosphere

■ Physical properties:

- ▶ **Sedimentary basin:** $\rho^s = 1\ 200 \text{ kg.m}^{-3}$, $c_p^s = 3\ 400 \text{ m.s}^{-1}$, $c_s = 1\ 400 \text{ m.s}^{-1}$
- ▶ **Bedrock:** $\rho^s = 5\ 350 \text{ kg.m}^{-3}$, $c_p^s = 3\ 090 \text{ m.s}^{-1}$, $c_s = 2\ 570 \text{ m.s}^{-1}$
- ▶ **Air:** $\rho^F := 1.292 \text{ k.m}^{-3}$, $c_p^F := 340 \text{ m.s}^{-1}$

■ Computational setting:

- ▶ **HHO-SDIRK(3,4) scheme**
- ▶ **Computational parameters:** $k = 1$, $\ell = 8$, and $n = 9$
- ▶ **homogeneous Dirichlet boundary conditions**
- ▶ **Initial condition:** velocity Ricker wavelet centered at the point $(x_c, y_c) \in \Omega^s$,

Propagation of an elastic pulse in a sedimentary basin and atmosphere

■ Physical properties:

- ▶ **Sedimentary basin:** $\rho^s = 1\ 200 \text{ kg.m}^{-3}$, $c_p^s = 3\ 400 \text{ m.s}^{-1}$, $c_s = 1\ 400 \text{ m.s}^{-1}$
- ▶ **Bedrock:** $\rho^s = 5\ 350 \text{ kg.m}^{-3}$, $c_p^s = 3\ 090 \text{ m.s}^{-1}$, $c_s = 2\ 570 \text{ m.s}^{-1}$
- ▶ **Air:** $\rho^F := 1.292 \text{ k.m}^{-3}$, $c_p^F := 340 \text{ m.s}^{-1}$

■ Computational setting:

- ▶ **HHO-SDIRK(3,4) scheme**
- ▶ **Computational parameters:** $k = 1$, $\ell = 8$, and $n = 9$
- ▶ **homogeneous Dirichlet boundary conditions**
- ▶ **Initial condition:** velocity Ricker wavelet centered at the point $(x_c, y_c) \in \Omega^s$,

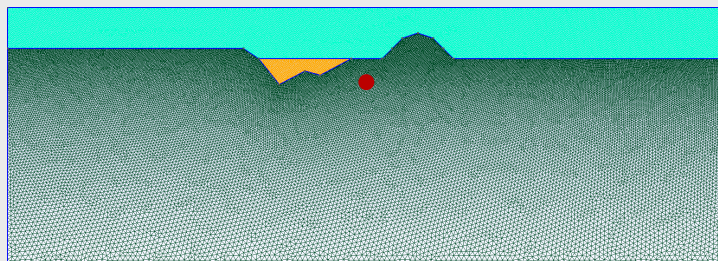


Fig. 15: Mesh of the sedimentary basin

Propagation of an elastic pulse in a sedimentary basin and atmosphere

- Energy transfer enhancement above the sedimentary basin

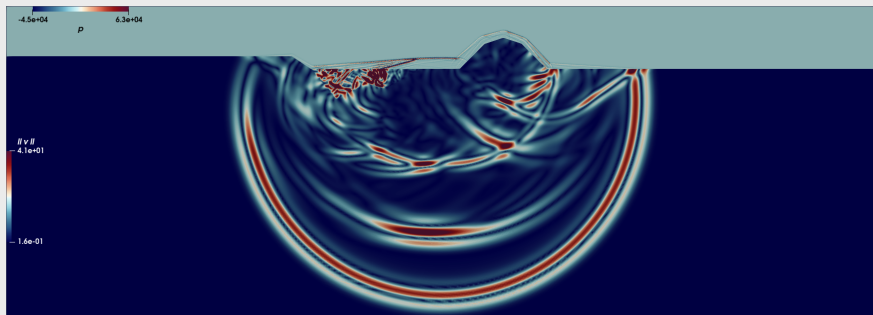


Fig. 16: Propagation of an elastic pulse in a sedimentary basin and atmosphere

Table of Contents

- 1 Motivation
 - Context and issues
 - Introduction to dG and HDG/HHO methods
- 2 Model problem
- 3 RK-HHO discretization
 - HHO space semi-discretization
 - Singly diagonally implicit schemes
 - Explicit schemes
- 4 Numerical results
 - Convergence rates
 - Ricker wavelet
 - Sedimentary basin
- 5 To go further: Unfitted HHO method

Unfitted meshes

■ **Goal:** Simplify mesh generation

■ **Principle:** Meshing in the simplest possible way (Cartesian meshes)

Discontinuities are described using level set functions which cut the mesh cells.
The interfaces are taken into account by Nitsche's method without the use of Lagrange multipliers.

Issues

■ **Drawback:** Ill - conditioning

Some cells can have an arbitrarily small cut.

■ **Stabilization techniques:**

- ▶ Agglomeration [Burman, Cicuttin, Delay, Ern, 2021]
 - The challenge lies in the modification of the mesh:
Hardly compatible with HPC architectures
- ▶ Discrete extension [Burman, Hansbo, Larson, 2020/2021]
 - The challenge lies in the modification of the scheme

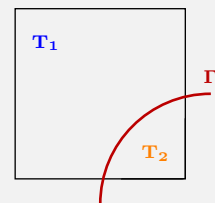


Fig. 17: Exemple of a bad cut

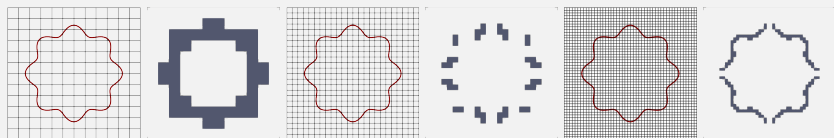


Fig. 18: Agglomeration procedure for different mesh refinement levels for a flower interface

Goal of the present work

Derive a new **unfitted HHO method** with **discrete polynomial extension compatible with HPC architecture**.

Elliptic interface problem

$$\begin{cases} -\nabla \cdot (\kappa \nabla u(t)) = f(t) & \text{in } \Omega_1 \cup \Omega_2, \\ [u(t)]_\Gamma = g_D & \text{on } \Gamma, \\ [\kappa \nabla u(t)]_\Gamma \cdot \mathbf{n}_\Gamma = g_N & \text{on } \Gamma, \\ u(t) = 0 & \text{on } \partial\Omega, \end{cases}$$

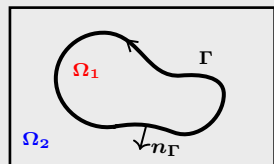


Fig. 19: Model problem

Partitioning of the unfitted mesh

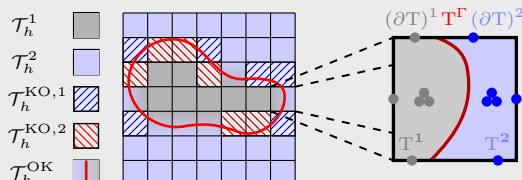


Fig. 20: Left panel. Illustration of the different type of cell involved in the unfitted mesh.
Right panel. Zoom on a cut cell.

Pairing operator

$$\mathcal{N}_i : \mathcal{T}_h^{\text{KO}, i} \ni T \longmapsto S \in (\mathcal{T}_h^i \cup \mathcal{T}_h^{\text{OK}} \cup \mathcal{T}_h^{\text{KO}, \bar{i}})$$

$$\mathcal{T}_h^{\text{KO}, i} = (\mathcal{T}_h^{\text{KO}, i} \cap \mathcal{N}_i^{-1}(\mathcal{T}_h^i)) \cup (\mathcal{T}_h^{\text{KO}, i} \cap \mathcal{N}_i^{-1}(\mathcal{T}_h^{\text{KO}, \bar{i}})) \cup (\mathcal{T}_h^{\text{KO}, i} \cap \mathcal{N}_i^{-1}(\mathcal{T}_h^{\text{OK}}))$$

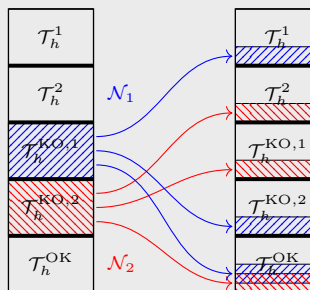


Fig. 21: Representation of the distribution of paired cells by the bad cut cells.

Pairing operator

$$\mathcal{N}_i : \mathcal{T}_h^{\text{KO}, i} \ni T \longmapsto S \in (\mathcal{T}_h^i \cup \mathcal{T}_h^{\text{OK}} \cup \mathcal{T}_h^{\text{KO}, \bar{i}})$$

$$\mathcal{T}_h^{\text{KO}, i} = (\mathcal{T}_h^{\text{KO}, i} \cap \mathcal{N}_i^{-1}(\mathcal{T}_h^i)) \cup (\mathcal{T}_h^{\text{KO}, i} \cap \mathcal{N}_i^{-1}(\mathcal{T}_h^{\text{KO}, \bar{i}})) \cup (\mathcal{T}_h^{\text{KO}, i} \cap \mathcal{N}_i^{-1}(\mathcal{T}_h^{\text{OK}}))$$

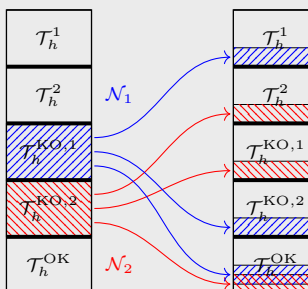


Fig. 21: Representation of the distribution of paired cells by the bad cut cells.

Modification of the numerical scheme

- The different HHO operators are modified depending on the type of cell considered.
- The numerical analysis of this new scheme and its implementation are in progress.

Thank you for your attention